

Comparison of the Wave Energy Transport at the Cornets p/Halley and p/Giacobini-Zinner

A. Söding¹, K.-H. Glassmeier², S. A. Fuscher³, Fritz M. Neubauer⁴, and B. T. Tsurutani⁴

¹Institut für Geophysik und Meteorologie, Universität zu Köln, Albertus Magnus Platz, 50923 Köln, Germany

²Institut für Geophysik und Meteorologie Technische Universität Braunschweig, Mendelssohnstr. 3, 38106 Braunschweig, Germany

³Dept. 9120 Bldg 225, Lockheed Palo Alto Research Corp. 3251 Hanover St., Palo Alto, CA 94304-1191, USA

⁴JPL, 4800 Oak Grove Dr MS 169-506, Pasadena, CA 91109, USA

October 18, 1995

Abstract. Using magnetic field, plasma density and flow observations from spacecraft flybys of two comets, Elsässer variables are determined in order to study wave propagation directions. We investigated the inbound path of the Giotto spacecraft flyby of comet p/Halley outside the bow shock (between 10:36 and 19:11 UT on March 13, 1986, corresponding to distances from 3.1×10^6 km to 1.7×10^6 km from the nucleus) and the inbound and outbound path of the ICE spacecraft flyby of comet p/Giacobini-Zinner outside of the bow wave (between 00:00 and 9:24 UT and between 12:25 and 23:00 UT on September 11, 1985, corresponding to distances from 8.5×10^5 – 1.2×10^5 km from the nucleus and from 1.0×10^5 – 9.3×10^5 km from the nucleus, respectively). The interaction of cometary pickup ions and the solar wind is expected to generate waves propagating mostly antiparallel to the background magnetic field. The predicted wave propagation combined with observed wave modes generated by the ion cyclotron resonant, in which

they are compared with observed wave properties. Three modes are possible: right-hand polarized waves propagating toward the Sun (RH^+) and left-hand polarized waves propagating toward (LH^-) and away from the Sun (LH^+). Plasma conditions dictate that the RH^+ mode is the most unstable mode and we find satisfactory agreement between observed and predicted energy flow directions in regions outside the bow shock at Halley and the bow wave at Giacobini-Zinner, where local cometary ion pickup conditions dominate.

1 Introduction

In 1985 and 1986, ICE and Giotto had their rendezvous with the comets Giacobini-Zinner (G-Z) and Halley, respectively. Analysis of the data from these encounters has resulted in significant advances in the understanding of plasma processes near active comets (see for example the reviews of Neubauer (1990) and Tsurutani (1991)).

Mass loading of the solar wind by cometary ions is the main interaction process in the outer cometary at-

mosphere and the solar wind. Neutrals sublimated from the comet surface drift away from the comet with a velocity of about 1 km/s (Keller, 1976). The neutrals are ionized by photoionization or by charge exchange with solar wind ions. The typical timescale for ionization at 1 AU is of the order of 106s. Thus, an extended ionization region is produced. In the solar wind frame the newborn ions stream toward the Sun with the solar wind velocity $|\mathbf{v}|$. Due to the Lorentz force, the cometary ions are accelerated perpendicular to \mathbf{B} and gyrate around \mathbf{B} . In the solar wind frame they form a ring beam distribution traveling upstream at an initial angle given by

$$\cos \alpha = \frac{\mathbf{v} \cdot \mathbf{B}}{|\mathbf{v}| \cdot |\mathbf{B}|} \quad (1)$$

where α is the angle between the interplanetary magnetic field \mathbf{B} and \mathbf{v} with $0^\circ \leq \alpha \leq 90^\circ$. This beam is unstable and leads to the generation of plasma waves. These waves propagate parallel and antiparallel to \mathbf{B} :

The waves interact resonantly with the pick-up ions via the Doppler-shifted ion cyclotron resonance (Tsurutani and Smith, 1986). The initial ring beam distribution of the pick-up ions will be scattered to a spherical distribution in velocity space by this wave-particle interaction. During this process the ions will lose energy which becomes available for wave growth. The energy difference between the ring beam and the spherical distribution is called free energy and is non-linearly released as wave energy as shown by Budden and Johnstone (1992) for the comet Halley.

In the present paper we use Elsässer variables to calculate the specific energy densities of waves propagating in opposite directions. This study is based on the assumption that the waves are Alfvénic (non compressive). Using a description of the wave generation under local plasma conditions and based on the ion cyclotron resonance (Thorne and Tsurutani, 1987), predicted and observed energy transport are compared. A case study of this had been already done for Halley (Söding et al., 1995). Here, we compare the results from the Halley encounter with new results from the G-Z encounter.

2 Wave energy transport

Elsässer (1950) introduces variables to simplify the magnetohydrodynamic equations. These Elsässer variables are defined by (Cravens et al., 1989)

$$\mathbf{Z}^\pm = \mathbf{v} \pm \mathbf{v}_A \quad (2)$$

where \mathbf{v}_A denotes the vector Alfvén velocity. For a homogeneous and incompressible plasma, \mathbf{Z}^\pm describe the two possible Alfvénic wave modes propagating in opposite directions which may possibly interact non-linearly with each other. Each wave mode could have a different origin, so it is possible to investigate the evolution of two different physical processes.

Shear Alfvén waves propagate parallel and antiparallel to the magnetic field \mathbf{B} at the Alfvén speed. Therefore the Alfvén relation $\mathbf{Z}^\pm = \text{const.}$ characterizes waves propagating parallel to the background magnetic field \mathbf{B}_0 and $\mathbf{Z}^\pm = -\text{const.}$ for antiparallel propagating waves.

In the undisturbed solar wind at 1 AU waves are most often observed to propagate away from the Sun (Belcher and Davis, 1979).

Here we used only the fluctuating part of the Elsässer variables $\delta Z^\pm = \delta \mathbf{v} \pm \delta \mathbf{v}_A$. The specific energy densities of the wave modes, the total energy density and the normalized cross helicity are defined by (Marsch and Mangeney, 1987)

$$E^\pm = \frac{1}{2} \delta Z^\pm \cdot \delta Z^\pm \quad (3)$$

$$E_{tot} = \frac{1}{2} (E^+ + E^-) \quad (4)$$

$$\sigma_c = \frac{E^+ - E^-}{E^+ + E^-} \quad (5)$$

Thus E^+ describes the energy density of wave propagating antiparallel to \mathbf{B}_0 and E^- vice versa if the ambient magnetic field is directed away from the Sun. E^+ describes the energy density of wave propagating towards the Sun and E^- away from the Sun.

The Elsässer ratio $R_E = E^-/E^+$ indicate the mean direction of the Alfvén waves. For $R_E > 1$ waves propagating parallel to \mathbf{B}_0 dominate and for $R_E < 1$ it is the opposite case. For $|\sigma_c| > 0.7$ there is one strong Alfvén wave and for $|\sigma_c| < 0.7$ there are two Alfvén waves propagating in opposite directions.

In our analysis we used data from the Giotto and the ICE spacecraft. For Halley data from the magnetometer (MAG) and the Johnstone plasma analyzer (JPA) are used (Neubauer et al., 1986, Johnston et al., 1986). The magnetic field and the plasma data as well are given as a 3 component vector, the temporal resolutions 8s and they are given in a Halley solar ecliptic (HSE) coordinate system. In this coordinate system, the X axis

points towards the Sun along the Sun-comet line, the Y axis is antiparallel to the direction of planetary orbital motion and the Z axis completes a right handed coordinate system.

For G-Z, data from the magnetometer and the solar wind electron instrument are used (Bame et al., 1986, Frandsen et al., 1978). The plasma parameters are based on 2-D electron measurements in the spin plane of ICE with a temporal resolution of 24s. The magnetic field data are averaged over the same interval, but they are given as a 3 component vector in a spacecraft centered solar ecliptic system. The X axis points toward the Sun and the Y axis toward dusk. The spin axis was perpendicular to the ecliptic within an accuracy of 0.5 degrees, thus defining the Z axis. Since two component plasma measurements only are available, all derived quantities for G-Z are determined in the spin plane X,Y only.

We have used only data upstream from the bow shocks. For Halley we investigate only the inbound leg. The bow shock is observed on March 13, 1986 at 19:23 UT corresponding to a distance of 1.15×10^6 km from the nucleus (Neubauer et al., 1986). We have investigated the region from 3.3×10^6 km to 1.2×10^6 km to the comet (from 10:36 UT to 19:08 UT). For G-Z the bow waves inbound and outbound are observed on September 11, 1985 at 9:30 UT and 12:20 UT, respectively corresponding to distances of 1.16×10^5 km and 0.96×10^5 km from the nucleus. Inbound we investigate the time interval between 00:00 UT and 9:24 UT (8.2×10^5 - 1.2×10^5 km) and outbound between 12:25 UT and 23:30 UT (1.1×10^5 - 9.3×10^5 km). The spatial scale for Halley is one or-

Table 1. Halley inbound path, $\text{sign}(\mathbf{B} \cdot \mathbf{v}) = +1$

Time	Distance in 10^6 [km]
10:57:22-11:00:42	3.21 - 3.20
11:34:10-11:59:46	3.06 - 2.93
12:03:54- 12:05:30	2.94 - 2.93
14:40:34- 14:49:54	2.30 - 2.26
14:53:38-15:24:26	2.24 - 2.12
15:31:22- 15:38:50	2.09 - 2.06
15:40:02-15:42:34	2.05 - 2.04
16:11:14- 19:08:02	1.92 - 1.20

Table 2. G-Z inbound path, $\text{sign}(\mathbf{B}_0) = +1$

Time	Distance in 10^3 [km]
00:00:49- 00:02:01	824-822
00:10:25-00:58:25	812 -75<
01:17:37-09:22:01	729- 126

der of magnitude greater than that for (1), the reason for this scale difference is the different gas production rates at the two comets, $Q = 2 \times 10^{28}$ molecule/s at 1.03 AU for G-Z (von Rosenvinge et al., 1986) and $Q = 7 \times 10^{29}$ molecules/s at 0.89 AU for Halley (Krankowsky et al., 1986).

Table 3. G-Z outbound path, $\text{sign}(\mathbf{B} \cdot \mathbf{v}) = -1$

Time	Distance in 10^3 [km]
12:28:36- 12:57:00	107- 142
13:01:48-15:15:24	148-314
15:17:48 - 16:36:36	317- 415
16:51:00 - 17:01:24	433-446
17:56:12-18:18:12	514-547
19:37:00-19:43:24	640- 648
19:47:48-19:51:24	652-658
20:37:48-23:30:12	716 - 930

At all three investigated passages the magnetic field primarily points away from the Sun. This is shown later by the sign of $\mathbf{B} \cdot \mathbf{v}$. The intervals and distances where \mathbf{B} is directed away from the Sun are given in the Tables 1, 2 and 3 for 8s and 24s averages, respectively. In the calculated spectra for Halley, \mathbf{B}_0 is directed towards the Sun only between 10:36 UT and 11:10 UT ($3.3 \times 10^6 - 3.2 \times 10^6$ km) and around 15:09 UT (2.2×10^6 km) and for the inbound leg of G-Z \mathbf{B}_0 is always directed away from the Sun. On the outbound path of G-Z except for 16:41 UT to 20:31 UT ($4.2 \times 10^5 - 7.1 \times 10^5$ km) \mathbf{B}_0 points away from the Sun.

To compute the energy density spectra we used 512 data points for the Fourier transform in the case of Halley and in case of G-Z 128 successive points with a running average over 5 and 3 estimates, respectively.

In Fig. 1 and Fig. 2 the specific and total energy densities, the Elsasser ratio and the normalized cross helicity integrated over the frequency range 1-3 mHz and 3-60 mHz as a function of the distance to the nucleus are shown. In the frequency range 1-3 mHz (Fig. 1) no influence depending on the distance to the comet is observed. $B^+ > B^-$ indicates that waves propagating parallel to \mathbf{B}_0 dominate. The total energy density is roughly constant. In the frequency range 3-60 mHz (Fig. 2) the influence of the comet is clearly visible. This is the frequency range at and above the gyro frequency of the water group ions (2-5 mHz during this interval). The energy density of waves propagating parallel to \mathbf{B}_0 is constant in this frequency range, but the energy density of the antiparallel waves increases during the approach.

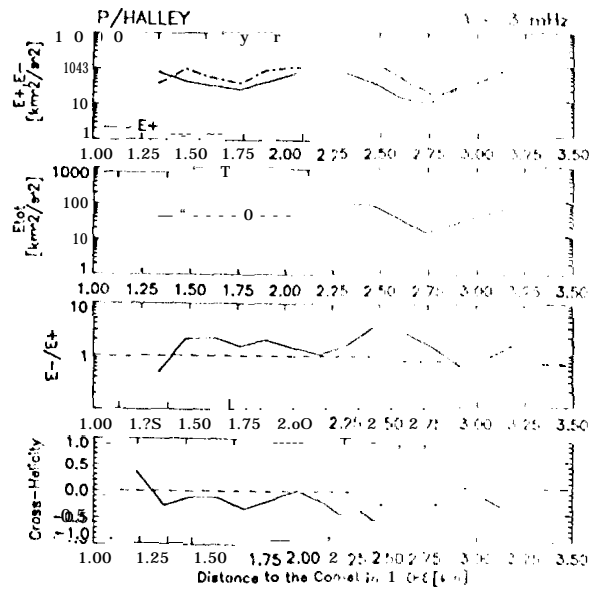


Fig. 1. Specific and total energy densities, Elsasser ratio and normalized cross helicity at comet Halley for the frequency range 1-3 mHz at the inbound. E^+ describes waves propagating antiparallel B_0 and E^- vice versa. No dependence of the distance is observed.

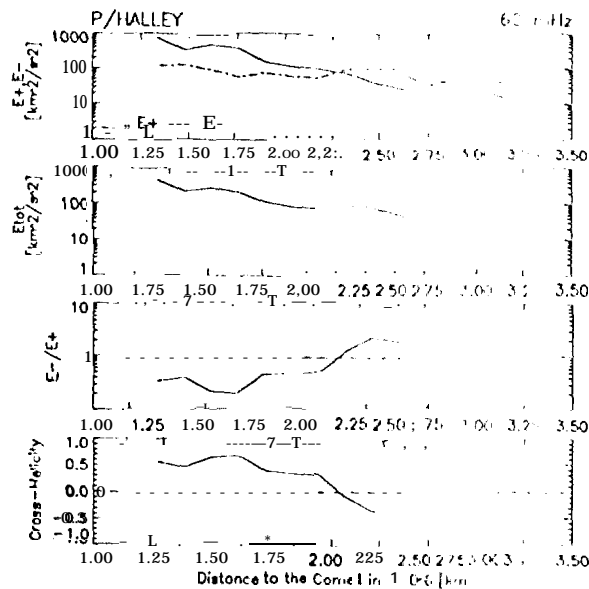


Fig. 2. As Fig. 1, but for the frequency range of 30 mHz above the gyro frequency of water group ions. A dependence of the distance is observable for E^+ , but not for E^- .

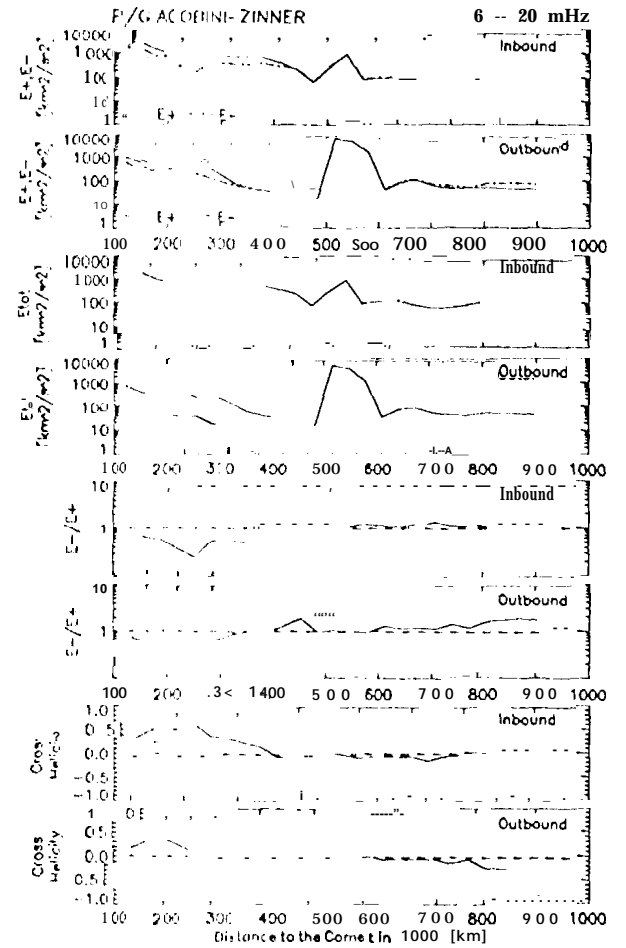


Fig. 3. As Fig. 1 but for the frequency range 6-20 mHz above the water group ion gyro frequency and both at the inbound and the outbound leg of Giacobini-Zinner.

Outside of 2.3, 10^6 km waves propagating away from the Sun (parallel to B_0) dominate and closer to the comet waves propagating toward the Sun (antiparallel to B_0) dominate. This dependence of the distance to the comet is also shown in the Elsasser ratio and in the normalized cross helicity. Close to the comet the cross helicity is relatively high (~ 0.6), but there are still two wave modes propagating in opposite directions. The increase of E_{tot} during the approach is due to the increase of E^+ .

For G-Z the results are not as clear as for Halley, but a similar dependence of the distance on both comets. The gyro frequency of the water group ions is about 7 mHz on the inbound and about 1 mHz on the outbound leg. In Fig. 3 the specific and total energy densities, the Elsässer ratio and the cross helicity for the range 6–20 mHz for both inbound and outbound are shown. Note that all the variables are calculated only in the spin plan and the part of the fluctuations outside the ecliptic plan are not taken into account. The same evolution is clearly visible for the inbound and the outbound path. Up to 450,000 km to the comet the following relations hold: $E^+ \approx E^-$, $R_E \approx 1$ and $|\sigma_c| \approx 0$. Assuming noncompressive waves, this result is explained by the presence of two oppositely propagating equal amplitude waves. On the other hand nonlinear compressive waves may perhaps give the same results. However, E^- tends to be a little bit higher than E^+ throughout this period. Closer to the comet the relations change to: $E^- > E^+$, $R_E < 1$ and $|\sigma_c| > 0$. In this case the increase of E_{tot} is carried by E^+ and E^- . Therefore close to the comet waves propagating towards the Sun dominate and far away from the comet waves propagating away from the Sun tend to be slightly more important.

The peak outbound around 550,000 km is caused by a decrease of B to 2.5 nT in this region.

In summary we observed the similar phenomenon for Halley and G-Z for fluctuations with frequency higher than the water group ion gyro frequency. At greater distances from the comets the dominant waves propagate parallel to the background magnetic field B_0 (which

points mostly outward from the Sun). In case of G-Z the specific energy density of these waves is only a slightly larger than that for the antiparallel waves. But closer to the comets the Elsässer ratio reverses. Up to distances of 2.3×10^6 km for Halley, 4.4×10^5 km inbound of G-Z and 3.9×10^5 km outbound of G-7, waves propagating antiparallel to B_0 dominate. Close to the comets B_0 is directed away from the Sun in all three cases in Fig. 2 and 3, so the most unstable waves are propagating towards the Sun. The cross helicity of G-Z is clearly smaller than for Halley close to the comet. The reduced cross helicity implies that waves propagating in opposite directions are generated at G-Z whereas antiparallel waves are more dominant at Halley. This effect is also seen in the increase of E^- during the approach at G-Z. Although the energy densities are compared at G-Z, in two dimensions only, they are 5 times bigger than at Halley, indicating that stronger waves were generated at G-Z compared to Halley (Tsurutani, 1991).

3 Observed and predicted wave properties

Due to the ion cyclotron instability the cometary ions interact resonantly with the plasma waves and will be scattered in pitch angles. Thorne and Tsurutani (1987) have provided a description for the conditions under which this occurs (see also Neubauer et al. (1993), Söding et al., 1995). Three wave modes are possible. In the solar wind frame, these are right-hand polarized waves travelling towards the Sun (RH^-) and left-hand polarized

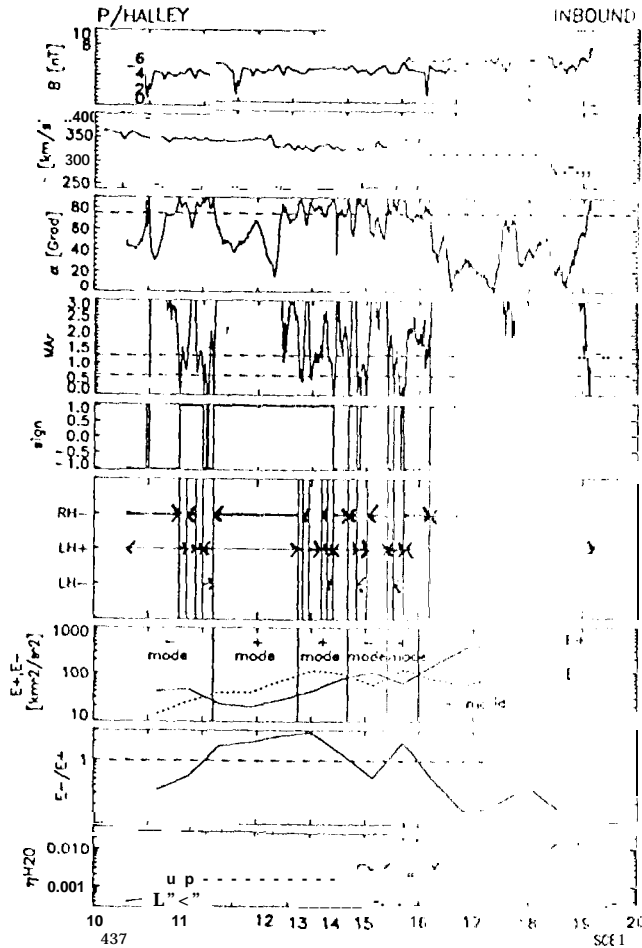


Fig. 4. The magnetic field magnitude B , the solar wind velocity v , θ , angle α , the Alfvén-Mach number M_{Ar} , the sign of $B \times v$ and the relative number density of heavy water group ions n_{H_2O} as a function of time are displayed for the inbound path of Halley upstream of the bow shock. One panel shows the presence of theoretically predicted RH^- , LH^+ and LH^- wave modes by presence of arrows. In the seventh and eighth panel are the specific energy densities E^+ of wave propagating towards and away from the Sun and the Elsässer ratio E^+/E^- shown. In fact of the observations expected wave modes are signed by "+" mode and "-" mode. See also text.

waves propagating towards (LH^-) and away from the Sun (LH^+).

From the ion cyclotron resonance condition together with a two component cold plasma model with solar wind protons and heavy water group cometary ions Thorne and Tsurutani (1987) obtain a resonance condition depending on the dimension-less field alignment Alfvén-Mach number $MA_r = v_{sw} \cos \alpha / v_A$. This condition depends also on the heavy ion mass m , and the relative number density of heavy ions η_4 . Near the bow shock of Halley $m_4 = 18$ (H_2O ions) and $\eta_4 \approx 10^{-2}$ were observed whereas of comet G-Z $m_4 = 18$ and $\eta_4 \approx 10^{-1}$. In

the interaction region of the comet with the solar wind η_4 decreases exponentially with increasing distance to the comet. This leads to constraints for the excitation of various wave modes. Resonant RH^- mode waves below a minimum value of M_{Ar} (which depends on η_4) are no longer excited. While for the LH mode no limitation on the excitation with respect to M_{Ar} exists. At the same time different wave modes can be generated. As these waves grow to large amplitudes and compete for the available free energy, the instability with the largest growth rate will survive.

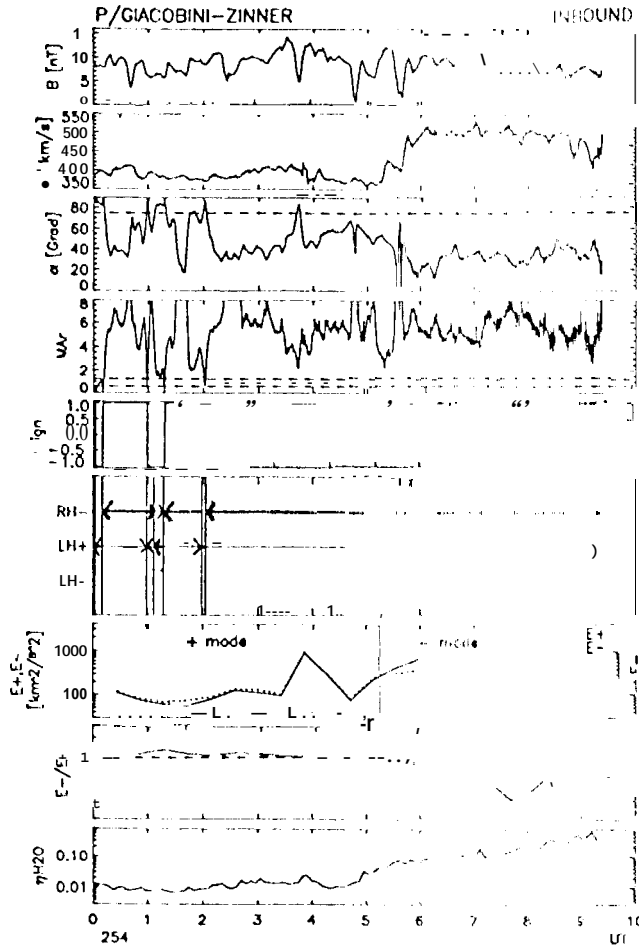


Fig. 5. As Fig. 4, but for the inbound path of Giacobini-Zinner. All variables are only calculated from two dimensions.

From Fig. 4 and 5 of Thorne and Tsurutani (1987) (see also Neubauer et al. (1993), Söding et al. (1994)) the conditions of theoretically predicted wave modes are follows: for Halley for $M_{Ar} > 1.25$ and for GZ for $M_{Ar} > 1.25$ RH^- mode exists and is always dominant for $30^\circ \leq \alpha \leq 75^\circ$; for $M_{Ar} < 0.6$ the LH^- mode will be excited; the LH^+ mode exists for any M_{Ar} except for $\alpha = 90^\circ$. Its wave growth rate is larger than that of the LH^- mode, if both are excited, and larger than that of the RH^- mode, if $\alpha \geq 75^\circ$. The Fig. 4,

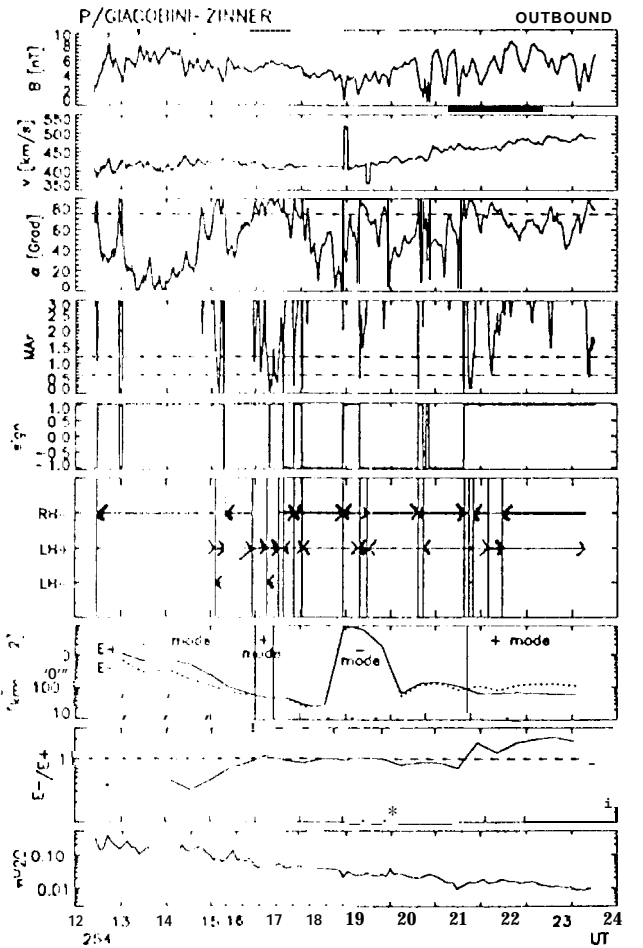


Fig. 6. As Fig. 5, but for the outbound path of Giacobini-Zinner.

5 and 6 show the magnitude of the magnetic field B , the solar wind velocity v , the angle α , the field aligned Alfvén-Mach number M_{Ar} , the sign of $B \cdot v$. In case of $sign(B \cdot v) = +1$ the magnetic field is directed away from the Sun and vice versa for $sign(B \cdot v) = -1$. In the lower panel the relative number density of heavy water groups n_{H_2O} is shown. For the calculations we used the model of Huddleston et al. (1990). The sixth panel indicates the presence of the theoretically predicted wave modes RH^+ , LH^+ and LH^- by the arrows. LH^+ describes a wave mode propagating away from the Sun and

RH and LH^- towards the Sun. The bold arrows have the largest wave growth rate and are therefore, wave mode expected to dominate. Arrows pointing from right to left are antiparallel to B_0 and arrow from left to right parallel. Two other panels display the specific energy densities E^\pm and the Elsässer ratio $\frac{E^+}{E^-}$ for the frequency range 3-60 MHz in case of Halley and 6-10 MHz in case of G-Z. To compare the predicted wave mode with E^\pm with respect to the Sun, it is necessary to use $-B$ instead of B , if the radial component of B is directed towards the Sun. The times where this happens are indicated in the sign panel and have been mentioned above. The expected wave mode are marked with “+ mode” if $E^- > E^+$ and with “- mode” if $E^+ > E^-$ in these panels.

The results of Fig. 4 at Halley are briefly summarized here, since they have been described in detail in Söding et al. (1995). In general observed and predicted energy flow directions agree, except between 15:07 and 15:56 UT where there is a clear disagreement: in this interval, the observed is a “+” mode and predicted a “-” mode. During this time in the water group distribution the ions are not observed at the local point of pick up, Söding et al. (1995) conclude that the Naves have been generated under pick-up conditions that were different from the local observed conditions.

During the inbound trajectory at G-Z (Fig. 5) the RH mode is expected to be excited during the intervals 00:10-1:59 and 2:03-9:24 UT and it always has the largest wave growth rate except between 1:07 and 1:17 UT. Only between 00:00 and 01:10 UT, 1:07 and 1:17

UT and 1:59 and 2:03 UT the LH^+ mode is expected to be the dominant one. The LH^- mode should never be excited. The observations show a “-” mode between 5:15 and 8:58 UT and a “+” mode during times before. Indeed in case of noncompressive waves the Elsässer ratio indicates in the earlier region the existence of two wave modes with opposite propagation directions, but with nearly the same energy densities. The theoretical prediction and the observations agree only in the region close to the comet where the “-” mode is observed. Further away when $E^+ \approx E^-$ no agreement is found.

On the outbound path of G-Z (Fig. 6) the situation is more complicated. The RH is expected during the time intervals 12:28-15:07, 15:19-15:56, 16:31-20:44 and 20:53-23:17 UT. Only during 16:31-16:37, 18:19-18:28 and 21:09-21:28 UT the RH^- mode does not have the largest growth rate and is not expected to be dominant at these times. The LH^+ mode is expected to be excited and to be dominating between 15:07 and 15:19, 15:56 and 16:37, 18:19 and 18:28, 20:44 and 20:50 and 21:09 and 21:28 UT. The LH^- mode is only expected for 3 short time intervals. The observations show the “-” mode between 12:51 and 16:00 and 16:24 and 20:42 UT and the “+” mode during the interval 16:00-16:24 and 20:42-23:05 UT. For the observed “-” mode a clear agreement with the theory is found, also for the “+” mode between 16:00 and 16:24 UT. A discrepancy is observed during 20:42 and 23:05 UT.

Thus at G-Z like at Halley, there is agreement between observations and predictions in the regions close to the comet. But the question arises, why at G-Z only

inside of 433,000 km (5:15 UT) inbound and inside of 720,000 km (20:42 UT) outbound?

The relative number of the heavy water group ions η_{H_2O} shows a dependence of the distance to the comet which can answer these questions. Between 00:00 and 5:00 UT inbound and 20:30 and 23:30 UT outbound η_{H_2O} is nearly constant. During further approach η_{H_2O} increases exponential. For this time interval we found the correspondence of the predicted and observed wave modes. This implies that the region of the influence of the comet to the generation of waves is limited through the noticeable increase of η_{H_2O} . Outside of this time influence of the pick-up ions could be neglected and the fluctuations may be intrinsic to the undisturbed solar wind. These fluctuations are most often propagating away from the Sun (Belcher and Davis, Jr., 1971).

Similar studies have been done at p/Giotto/Skjeldrup, where the plasma conditions are quite different than at Halley and G-Z. Neubauer et al. (1993) predicted RH^- and LH^+ modes upstream of the bow shock and Glassmeier and Neubauer (1993) observed, in left-hand-polarized waves in these regions in the peak spectral power, the magnetic field.

4 Discussion and Summary

The regions upstream of the bow shock in the neighbourhood of Giotto to comet p/Halley and the inbound and outbound legs of ICE to comet p/G-Z are compared with respect to wave energy transport. During all three intervals similar plasma conditions are observed. Close to the

bow shock the magnetic field is quasi-parallel ($\alpha < 45^\circ$) and it is further outside quasi-perpendicular ($\alpha > 45^\circ$). This indicates that one expects similar waves and similar waves are observed.

The specific energy densities E^\pm , the total energy density E_{tot} , as well as the Elsässer ratio and the cross helicity for frequencies higher than the gyro frequency have the same dependence on the distance to the nucleus at the two comets but on different scales. The factor of 35 greater gas production rate at Halley compared to G-Z produces an interaction region that is a factor 10 larger. In the interaction regions, mostly waves propagating antiparallel to B_0 are generated with B_0 pointing away from the Sun. This is clearly seen during the whole region investigated, but also at G-Z for distances closer than 4.4×10^5 km inbound and 3.9×10^5 km outbound. Further outside of G-Z the energy density of the fluctuations propagating in opposite directions are nearly the same and the influence of the comet could be neglected.

The comparison of the observed wave energy transport directions with the predicted RH^- , and LH^+ and LH^- modes owing to the ion cyclotron resonance indicates in general a good agreement inside of the influence region of the comet. In all three passages the RH^- mode have been driven unstable by the pick-up ion instability. The analysis of the Elsässer variables leads to regions of influence at G-Z up to 4.3×10^5 km inbound and 7.2×10^5 km outbound and at the inbound path of Halley up to 4.4×10^5 km which was previously investigated.

Acknowledgement. We thank R.V. Stein for helpful discussions. Also we thank Alan Johnstone for the use of the (at, f, th? if), and the members of the experiments for the support of the magnetometer and the JPA experiments on Giotto and other magnetometer and plasma experiments on K. Y. The work by A. S., K.H.G. and F.M.N. was supported financially by DARA research at Lockhead was funded by the independent Research Program. The work by B.T.T. was done at the Jet Propulsion Laboratory under contract with the NASA.

References

- Bame, S. et al., Comet Giacobini-Zinner Plasma description, *Science*, 232, 3563-361, 1986.
- Belcher, J. and L. Davis, Jr., Large amplitude Alfvén waves in the interplanetary medium, 2, *J. Geophys. Res.*, 76(16), 3534, 1971.
- Elsässer, W., The hydromagnetic equations *Phys. Rev. A*, 79, 183, 1950.
- Frandsen, A., B. Connor, J. Amisloot, and E. Smith, The ISEE-C vector 1, < minimum magnetometer, *IEEE Trans. Geosci. Electron.*, GE-16, 195, 1978.
- Glassmeier, K. and F. Neubauer, Low frequency electromagnetic plasma waves at comet P/Grigg-Skjellerup Overview and spectral characteristics, *J. Geophys. Res.*, 98(9), 936, 1993.
- Huddleston, L., A. Johnstone, and A. Coates, Determination of comet Halley gas emission characteristics from mass loading of the solar wind, *J. Geophys. Res.*, 95(A1), 21-30, 1990.
- Huddleston, D. E. and A. D. Johnstone, Relationship between wave energy and free energy from pickup ions in the comet Halley environment, *J. Geophys. Res.*, 97(12), 217-2230, 1992.
- Johnstone, A. et al., Ion Row at comet Halley, *Nature* 321, 344-347, 1986.
- Keller, H., Interpretation of ultraviolet observations of comets, *Space Sci. Rev.*, 18, 641, 1976.
- Kranowsky, D. et al., In situ gas and ion measurements at comet Halley, *Nature*, 321, 326-329, 1986.
- Marsch, E. and A. Mangeney, Ideal MHD equations in terms of compressive Elsässer variables, *J. Geophys. Res.*, 92(A7), 7363-7367, 1987.
- Neubauer, F. M. K. H. Glassmeier, A. J. Coates, et al., Low frequency electromagnetic plasma waves at comet P/Grigg-Skjellerup: Analysis and interpretation, *J. Geophys. Res.*, 98(A12), 20,937-20,953, 1993.
- Neubauer, F. M., K.-H. Glassmeier, M. Pohl, et al., First results from the Giotto magnetometer experiment at comet Halley, *Nature*, 321(6067), 352-355, 1986.
- Neugebauer, M., Spacecraft observations of the interaction of active comets with the solar wind, *Rev. Geoph.*, 28(2), 231, 1990.
- Söding, A., K.-H. Glassmeier, A. Johnstone, and F. Neubauer, Pick-up ions and associated wave energy transport at comet P/Halley: A case study, *Geophys. Res. Lett.*, in press, 1995.
- Thorne, R. M. and B. T. Tsurutani, Resonant interactions between cometary ions and low frequency electromagnetic waves, *Planet. Space Sci.*, 35(12), 1501-1508, 1987.
- Tsurutani, B. T., 1991. Comets: A laboratory for plasma wave instabilities In A. D. Johnstone (Ed.), *Cometary Plasma Processes*, *Geophys. Monogr. Ser.*, Volume 61, Washington D. C., pp 189-210. AGU.
- Tsurutani, B. T. and E. J. Smith, Hydromagnetic waves and instabilities associated with cometary ion pickup: ICE observations, *Geophys. Res. Lett.*, 13, 263-266, 1986.
- Tu, C.-Y., E. Marsch, and K. Thiemé, Basic properties of solar wind MHD turbulence near 0.3 AU analyzed by means of Elsässer variables, *J. Geophys. Res.*, 94(A9), 11,739-11,759, 1989.

